Interactions of Poly(amidoamine) Dendrimers with Human Serum Albumin: Binding Constants and Mechanisms

Jyotsnendu Giri,[†,#] Mamadou S. Diallo,[‡,§,*] André J. Simpson,[⊥] Yi Liu,[†] William A. Goddard, III,[†] Rajeev Kumar,[⊥] and Gwen C. Woods[⊥]

[†]Materials and Process Simulation Center, Division of Chemistry and Chemical Engineering, California Institute of Technology, [‡]Graduate School of Energy, Environment, Water and Sustainability (EEWS), Korea Advanced Institute of Science and Technology (KAIST), [§]Environmental Science and Engineering, Division of Engineering and Applied Science, California Institute of Technology, and [⊥]Department of Chemistry, University of Toronto at Scarborough. [#] Present Address: Polymer Division (Biomaterials Group), National Institute of Standards and Technology.

ABSTRACT The interactions of nanomaterials with plasma proteins have a significant impact on their *in vivo* transport and fate in biological fluids. This article discusses the binding of human serum albumin (HSA) to poly(amidoamine) [PAMAM] dendrimers. We use protein-coated silica particles to measure the HSA binding constants (K_b) of a homologous series of 19 PAMAM dendrimers in aqueous solutions at physiological pH (7.4) as a function of dendrimer generation, terminal group, and core chemistry. To gain insight into the mechanisms of HSA binding to PAMAM dendrimers, we combined ^{1}H NMR, saturation transfer difference (STD) NMR, and NMR diffusion ordered spectroscopy (DOSY) of dendrimer–HSA complexes with atomistic molecular dynamics (MD) simulations of dendrimer conformation in aqueous solutions. The binding measurements show that the HSA binding constants (K_b) of PAMAM dendrimers depend on dendrimer size and terminal group chemistry. The NMR ^{1}H and DOSY experiments indicate that the interactions between HSA and PAMAM dendrimers are relatively weak. The ^{1}H NMR STD experiments and MD simulations suggest that the inner shell protons of the dendrimers groups interact more strongly with HSA proteins. These interactions, which are consistently observed for different dendrimer generations (G0-NH_2 *vs* G4-NH_2) and terminal groups (G4-NH_2 *vs* G4-OH with amidoethanol groups), suggest that PAMAM dendrimers adopt backfolded configurations as they form weak complexes with HSA proteins in aqueous solutions at physiological pH (7.4).

KEYWORDS: dendrimers · proteins · human serum albumin · nanobiotechnology · nantoxicology · NMR epitope mapping and atomistic molecular dynamics simulations

Through the manipulation and control of the properties of matter at the molecular and supramolecular levels, nanotechnology is enabling major advances in a variety of fields including computing, energy generation, water purification, and medicine. Despite its great potential to improve human lives and the global economy, there is a growing concern that nanotechnology could also adversely impact human health and the environment.[1−3] Thus, a fundamental understanding of the interactions of engineered nanomaterials with biological macromolecules, cells, and organisms is critical to the development of sustainable nanotechnologies. It is well-known that xenobiotic compounds bind to proteins when they are in contact with biological fluids such as blood plasma.[4−7] The binding of nanoparticles (NPs) to proteins can significantly alter their *in vivo* transport and fate in biological fluids.[4−7]As pointed out by Cedervall *et al.*[8] and Lynch *et al.*,[9] the NPs might lose their intrinsic identities by behaving as protein-coated compounds. Moreover, the protein coatings on the surfaces of NPs often modulate their biological responses as they undergo conformational changes and/or dynamic exchanges with other proteins. Dawson and co-workers[10−12] have characterized the thermodynamics and kinetics of binding of polymeric NPs to proteins in human plasma using a broad range of analytical techniques including isothermal titration calorimetry, size-exclusion chromatography, and surface plasmon resonance. They reported the formation of two types of protein coatings on the surfaces of NPs: a soft corona (with fast protein exchange kinetics) and hard corona (with slow protein exchange kinetics). Dawson and co-workers[10−12] also found that NP size (*e.g.*, 50 nm *versus* 100 nm) and surface chemistry (*e.g.,* amine *versus* carboxylic) have significant effects on the compositions of the NP–protein coronas. In a more recent study, they concluded that plasma-derived protein coatings on the surface of polystyrene NPs (100–200 nm) and silica NPs (50 nm) are "sufficiently long-lived that, they, rather than the nanomaterial surface, are likely to be what the cell sees".[10−12] Note that the interactions

* Address correspondence to mdiallo@kaist.ac.kr, diallo@wag.caltech.edu.

Received for review August 20, 2010 and accepted March 25, 2011.

Published online March 25, 2011
10.1021/nn1021007

of proteins with NPs depend on their surface curvature. Very small NPs (*i.e.*, with highly curve surfaces) have been shown to suppress protein adsorption in some cases.[13] Thus, key unanswered questions are whether the observations and hypotheses of Dawson and coworkers[12] on the interactions of proteins with relatively large and hard NPs are applicable to smaller and softer organic nanostructures with size comparable to those of proteins.

Dendrimers are ideal model systems for probing the interactions of soft organic nanomaterials (NMs) with proteins in biological fluids. Dendrimers are highly branched 3-D globular and monodisperse nanostructures with controlled composition and architecture consisting of three components: a core, interior branch cells, and terminal branch cells.[14] Poly(amidoamine) (PAMAM) dendrimers were the first class of dendritic macromolecules to be commercialized.[14] They have been referred to as artificial proteins based on their similarity in size (*e.g.,* 2−13 nm in diameter), shape (*e.g.,* globular), electrophoretic mobility and hydrodynamic behavior.[14] The potential use of PAMAM dendrimers in biomedical applications such as gene therapy, drug delivery, and magnetic resonance imaging[14] make them good model systems for probing protein binding to NMs in biological fluids. Human serum albumin (HSA) is the most abundant protein (40 mg/mL) in the human blood circulatory system.[15,16] HSA binds and transports a broad range of compounds including metabolites, drugs, xenobiotic compounds, and nanomaterials. In this article, we combined experimental characterization and atomistic molecular dynamics (MD) simulations to probe the interactions of HSA with PAMAM dendrimers. We utilized protein-coated silica particles to measure the HSA binding constants (K_b) of a homologous series of 19 PAMAM dendrimers (Figure 1) in aqueous solutions at physiological pH (7.4) as a function of dendrimer generation, terminal group, and core chemistry. To gain insight into the mechanisms of HSA binding to PAMAM dendrimers, we combined ^{1}H NMR, saturation transfer difference (STD) NMR and NMR diffusion ordered spectroscopy (DOSY) investigations of complexes of dendrimer + HSA with atomistic molecular dynamics (MD) simulations of dendrimer conformation in aqueous solutions. The binding measurements show that the HSA binding constants (K_b) of PAMAM dendrimers depend on dendrimer size and terminal group chemistry. The ^{1}H NMR and DOSY experiments indicate that the interactions between HSA and PAMAM dendrimers are relatively weak. The NMR STD experiments and MD simulations suggest that the inner shell protons of the dendrimers and their neighboring amide groups interact more strongly with HSA proteins. These stronger interactions, which are consistently observed for different dendrimer generations (G0-NH_2 *vs* G4-NH_2) and terminal groups (G4-NH_2 *vs* G4-OH), suggest that PAMAM dendrimers adopt backfolded conformations as they form weak complexes with HSA proteins in aqueous solutions at physiological pH (7.4).

RESULTS AND DISCUSSION

Equilibrium dialysis, ultrafiltration, and ultracentrifugation are commonly used techniques to measure the binding of organic solutes to biological macromolecules in aqueous solutions.[17] The use of dialysis to measure the binding constants of dendritic macromolecules to proteins has yielded mixed results. Purohit *et al.*[18] employed dialysis (with a regenerated cellulose membrane of molecular weight cut off of 10 and 25 kDa) to measure the binding of a dendron (with 32 terminal amine groups and molecular weight 1.5−4.7 kDa) to HSA. They found that more than 50% of the dendrons (on a mass basis) were adsorbed onto the 10 kDa membrane. Our initial attempts to use dialysis to measure the binding constants of PAMAM dendrimers to HSA (using 10−30 kDa RC membrane) were not successful due to dendrimer adsorption to the RC membranes and limited diffusivity of PAMAM dendrimer through RC membrane (data not shown). Note that Shcharbin *et al.*[19] investigated the interactions between HSA and a G4-NH_2 PAMAM dendrimer [with ethylene diamine (EDA) core] using a suite of analytical techniques including zeta-potential measurements, capillary electrophoresis, isothermal titration calorimetry, circular dichroism (CD), and fluorescence spectroscopy. They reported that the binding affinity of PAMAM dendrimers to HSA depends on dendrimer generation and terminal group chemistry. The estimated binding constant (K_b) of a G4-NH_2 PAMAM using the different techniques varied by 2 orders of magnitude ranging from 10^3 to 10^5 M^{-1}.[19] Froehlich *et al.*[20] combined FT-IR, UV−visible, CD, and fluorescence spectroscopy to probe the binding of HSA to PAMAM dendrimers with ethylene diamine core and terminal amine groups (G4-NH_2) and terminal polyethylene glycol (PEG) groups [G3-PEG and G4-PEG] in aqueous solutions at physiological pH (7.4). They reported dendrimer−HSA binding constants (K_b) of $1.3 \pm 0.19 \times 10^5$ M^{-1} for G3-PEG, $2.2 \pm 0.4 \times 10^5$ M^{-1} for G4-PEG and $2.6 \pm 0.5 \times 10^5$ M^{-1} for G4-NH_2. Although these previous investigations have provided valuable information and insight into the interactions of PAMAM dendrimers with HSA, no consistent quantitative binding data were derived from these studies. Thus, one of the key objectives of this research was to measure the binding constants (K_b) of PAMAM dendrimers to HSA in aqueous solutions at physiological pH (7.4).

Binding Constant Measurements. In this study, we employed protein-coated TRANSIL beads from Sovicell[21] as alternative to dialysis to measure the binding constants (K_b) of PAMAM dendrimers (Figure 1) to HSA.

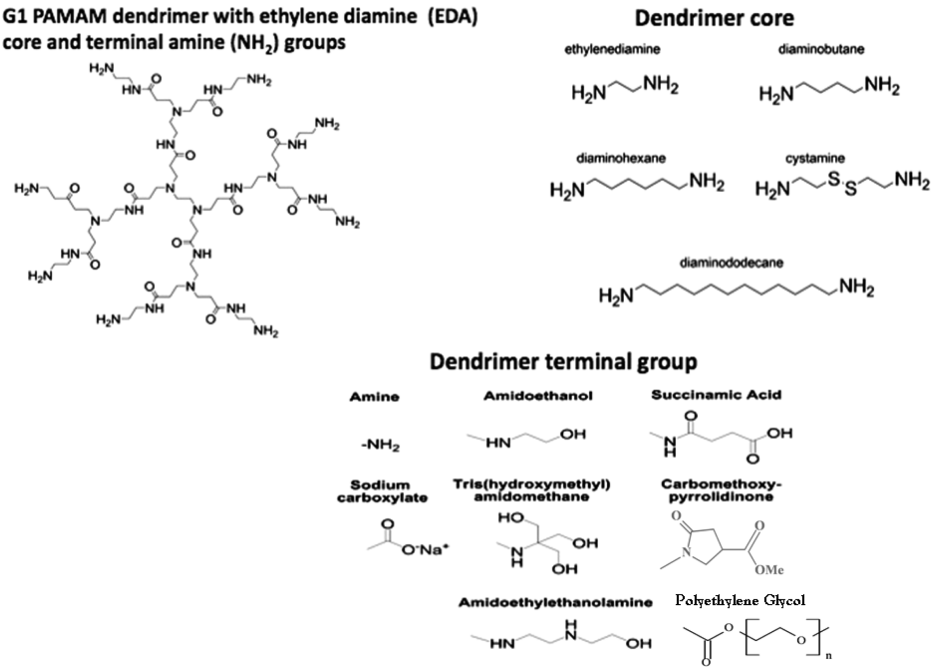

Figure 1. Core and terminal group chemistry of the PAMAM dendrimers evaluated in this study.

Solid-supported biomacromolecules are increasingly being utilized as (i) separation media for affinity chromatography and (ii) high-throughput bioassay systems.[22] The TRANSIL assay system has emerged as a versatile platform of solid-supported biomacromolecules for probing the interactions of solutes (*e.g.*, drugs, metabolites, and xenobiotic compounds) with lipid bilayers, plasma proteins,and membrane-bound proteins.[22] TRANSIL albumin kits consist of HSA proteins that are immobilized onto porous silica particles with average surface areas of ~10 m^2/g.[22] A typical SEM image of an HSA-coated silica particle is shown in Figure S1 of the Supporting Information (SI). In this case, a polymer cushion (with optimal chemistry, spacer length and coupling functionality) is first covalently attached to the surfaces of the silica particles before immobilization of the HSA proteins. The main purposes of this polymer cushion are to (i) shield the HSA proteins from the support, (ii) maintain the conformation integrity of the proteins, (iii) preserve the accessibility of the HSA binding sites, and (iv) eliminate nonspecific binding of solutes to the surfaces of the TRANSIL silica particles. Note that the selection of the TRANSIL-HSA binding assay was motivated by several considerations. First, TRANSIL beads have high HSA contents. Second, the polymer shields on the surfaces of the TRANSIL silica particles ensure that there is no significant difference between the conformations of free and immobilized HSA proteins.[22] Third, TRANSIL beads can be easily separated from aqueous solutions by centrifugation. Finally, we would like to point out that the TRANSIL albumin-binding assay was validated by Schumacher *et al.*,[23] They showed that the bound fractions (f_b) of various small drugs molecules to HSA that were measured using HSA-coated TRANSIL beads agree very well with those determined using dialysis.

TABLE 1. Binding Constant (K_b) and Selected Properties of PAMAM Dendrimers with Ethylene Diamine (EDA) Core and Terminal NH_2 Groups

generation	$N_{Terminal}$[a]	M_{wth} (Da)[b]	R_H (nm)[c]	K_b (M^{-1})
G0	4	517	0.96	$1.67 \pm 0.19 \times 10^5$
G1	8	1430	1.18	$2.83 \pm 0.78 \times 10^5$
G2	16	3256	1.47	$2.91 \pm 0.41 \times 10^5$
G3	32	6909	1.86	$3.65 \pm 0.75 \times 10^5$
G4	64	14215	2.44	$1.67 \pm 0.15 \times 10^6$
G5	128	28826	3.12	$3.10 \pm 1.0 \times 10^6$
G6	256	58048	3.81	$5.42 \pm 1.09 \times 10^6$
G8	1024	233383	4.76	$3.30 \pm 0.98 \times 10^6$

[a] $N_{Terminal}$: number of terminal groups. [b] M_{wth}: theoretical molar mass. [c] R_H: hydrodynamic radius.

Table 1 lists the measured HSA binding constants of G*x*-NH_2 PAMAM dendrimers with EDA core. We tested eight different dendrimer generations (G0, G1, G2, G3, G4, G5, G6 and G8). In these experiments, we varied the molar ratio of protein to dendrimer NH_2 groups from 0.01 to 0.1 by increasing the concentration of HSA (0.5 to 7.5 μM). By keeping the concentration of NH_2 groups constant at 64 μM for all G*x*-NH_2 PAMAM dendrimers, we were able to decouple the effects of size and terminal group concentration on their HSA binding constants. Figure 2 illustrates the effect of generation and size (as measured by the hydrodynamic radius) on the HSA binding constants (K_b) of PAMAM dendrimers. The corresponding fractional binding (FB) curve is plotted in Figure S2 of the SI. In all cases, each reported

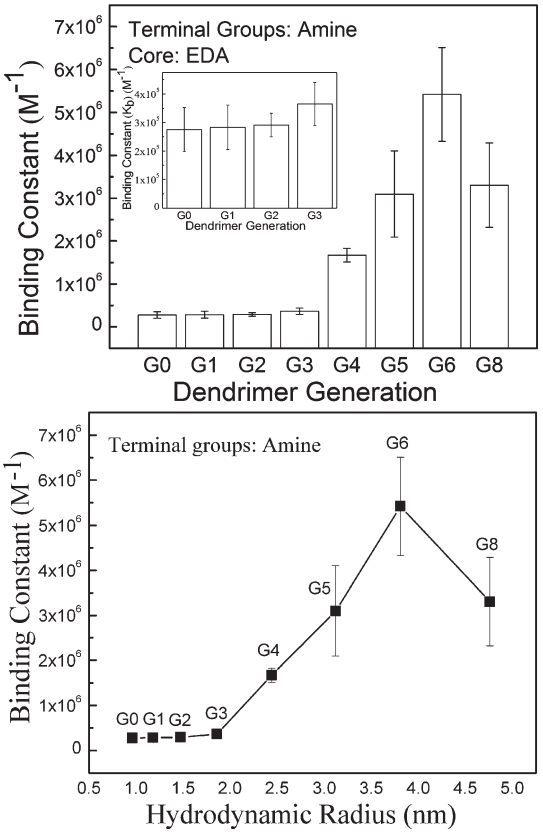

Figure 2. Effects of dendrimer generation and hydrodynamic radius on the binding constant (K_b) of PAMAM dendrimers with EDA core and terminal NH_2 groups at room temperature and pH 7.4. In all cases, the concentration of dendrimer NH_2 groups was kept constant at 64 μM.

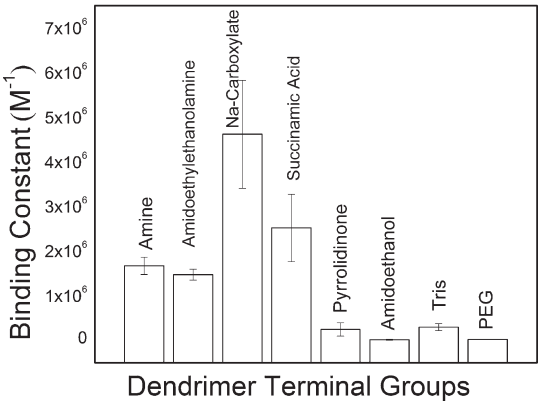

Figure 3. Effects of dendrimer terminal group on the HSA binding (K_b) of G4-X and G3.5-COONa PAMAM dendrimers at room temperature and pH 7.4. All the dendrimers have an ethylene diamine (EDA) core except the G4 dendrimer with amidoethylethanolamine terminal groups. This dendrimer has a diaminobutane (DAB) core. In all cases, the concentration of dendrimer terminal groups (X and COONa) was kept constant at 64 μM.

K_b value is the average of four measurements with different molar ratios of HSA to dendrimer NH_2 groups. Similarly, each reported error is the standard deviation of the average of the four measured K_b values. Figure 2 shows that the HSA binding constants of the G*x*-NH_2 PAMAM dendrimers (with EDA core) gradually increase with generation (from $1.67 \pm 0.19 \times 10^5$ for G0-NH2 to $5.42 \pm 1.09 \times 10^6$ for G6-NH_2) followed by a slight decrease ($3.30 \pm 0.98 \times 10^6$) for the G8-$NH_2$ dendrimer. Interestingly, the G6-NH_2 PAMAM dendrimer has the largest K_b value (Figure 2). We believe this might be the result of a size-based selective binding mechanism similar to that reported by Chiba *et al.*[24] They used a fluorescence-based competitive displacement assay to investigate the binding of G*x*.5 PAMAM dendrimers [with terminal COONa groups] to proteins including cytochrome-c and chymotrypsin. Chiba *et al.*[24] found that a dendrimer has a higher binding affinity toward a protein with comparable molecular surface area. For example, the G2.5 PAMAM dendrimer (with a molecular surface area of 1200 A^2) has the highest binding affinity to cytochrome-c, which has a molecular surface area of 1100 A^2. Similarly, the G3.5 PAMAM dendrimer (with a molecular surface area of 2250 A^2) has the highest binding affinity for chymotrypsin, which has a molecular surface area of 2400 A^2. As discussed by He *et al.*,[15] HSA folds into a heart-shaped 3-D structure that can be approximated by an equilateral triangular prism with sides of ~8 nm and height of ~3 nm. The similarity between the sizes of the sides of the HSA model triangular prism and the hydrodynamic diameter of the G6-NH_2 PAMAM dendrimer (7.62 nm) [Table 1] is consistent with the size selective binding mechanism observed by Chiba *et al.*[24] Note that this size-selective binding mechanism is also consistent with the nanoperiodic patterns of dendrimers (*i.e.*, quantized size effect) discussed by Tomalia.[25]

TABLE 2. Binding Constant K_b and Other Physical Parameters of PAMAM Dendrimers with Different Terminal Groups

generation	terminal group	$N_{Terminal}$[a]	M_{wth} (Da)[b]	K_b (M^{-1})
4	amine[c]	64	14215	$1.67 \pm 0.19 \times 10^6$
4	amidoethylethanolamine[d]	64	34492	$1.47 \pm 0.12 \times 10^6$
4	succinamic acid[c]	64	20619	$2.52 \pm 0.75 \times 10^6$
3.5	sodium carboxylate[c]	64	26252	$4.62 \pm 1.21 \times 10^6$
4	pyrrolidinone[c]	64	22285	$2.46 \pm 1.5 \times 10^5$
4	Tris[c]	64	18121	$2.95 \pm 0.77 \times 10^5$
4	amidoethanol[c]	64	14277	$1.29 \pm 0.93 \times 10^4$
4	Polyethylene glycol (PEG)[c]	64	49414	$1.77 \pm 0.28 \times 10^4$

[a] $N_{Terminal}$: number of terminal groups.. [b] M_{wth}: theoretical molar mass.. [c] Ethylenediamine core. [d] Diaminobutane core.

Figure 3 and Table 2 illustrate the effect of dendrimer terminal group chemistry on the binding constants (K_b) of PAMAM dendrimers to HSA. The corresponding fractional binding (FB) curve is plotted in Figure S3 of the SI. We evaluated eight different terminal groups: amine (NH_2), amidoethylethanolamine (EtNH), sodium carboxylate (COONa), succinamic acid (SA), pyrrolidinone (Pyro), amidoethanol (OH), tris(hydroxymethyl) amidomethane (Tris), and

polyethylene glycol (PEG). Except for the PAMAM dendrimer with sodium carboxylate terminal groups (G3.5), all dendrimers were fourth generation (G4) and thus have similar size and same number of tertiary amine and amide groups. Here again, we kept the concentration of dendrimer terminal groups constant at 64 μM for all the G4-X and G3.5 PAMAM dendrimers. This enabled us to decouple the effects of terminal group chemistry and concentration on the HSA binding constants of PAMAM dendrimers. Figure 3 and Table 2 show that the lowest K_b values are observed for the G4 PAMAM dendrimers with neutral terminal groups. The lower HSA binding constants of the G4-X PAMAM dendrimers with neutral (OH, PEG, and Pyro) terminal groups are consistent with a binding mechanism involving weak interactions (*e.g.,* hydrogen bonding) between dendrimer terminal groups and the protein amino acid residues. Enhanced hydrogen bonding could be the reason why the HSA binding constant of the dendrimer with Tris terminal groups (G4-Tris) is larger than that of the G4-OH dendrimer. Note that even though both dendrimers have the same total concentration of OH groups, the G4-Tris PAMAM dendrimer has 64 × 3 = 192 terminal OH groups that provide more sites for hydrogen bonding with the HSA protein.

Figure 3 and Table 2 also show that the HSA binding constants (K_b) of the PAMAM dendrimers with anionic and cationic terminal groups are significantly larger than those of the dendrimers with neutral terminal groups. These larger K_b values are consistent with a binding mechanism involving both electrostatic and hydrophobic interactions between the dendrimers and HSA amino acid residues. For the G*x*-NH_2 PAMAM dendrimers, our postulated mechanisms of binding with HSA are consistent with the electron paramagnetic resonance (EPR) studies by Ottaviani *et al.*[26] They employed continuous wave (CW) and electron-spin echo (ESE) EPR to probe the interactions of G2-NH_2 and G6-NH_2 PAMAM dendrimers (labeled with nitroxides) with selected amino acids (Gly, Glu, Arg, and Leu) and proteins (chymotrypsin and HSA) in aqueous solutions (D_2O). By varying the pH and extent of protonation of the dendrimers, Ottaviani *et al.*[26] showed that the binding of the G*x*-NH_2 PAMAM dendrimers to the amino acids, chymotrypsin and HSA is "mainly promoted when both electrostatic and hydrophobic interactions take place".

Not surprisingly, the K_b value of the G4-EtNH PAMAM dendrimer (1.47 ± 0.12 × 10^6 M^{-1}) is comparable to that of the G4-NH_2 PAMAM dendrimer (1.67 ± 0.19 × 10^6 M^{-1}). This dendrimer has 64 secondary amine (NH) groups (Figure 1) that are protonated at pH 7.4. Figure 3 and Table 2 show that the G3.5 PAMAM with terminal carboxlic groups has the highest K_b (4.62 ± 1.21 × 10^6 M^{-1}) among the PAMAM dendrimers with different terminal group chemistry. This value is approximately 2 times larger than that of the G4-NH_2 dendrimer (1.67 ± 0.15 × 10^6 M^{-1}). We attribute the larger HSA binding affinity of the G3.5 PAMAM to interactions between the terminal carboxylic groups groups of the dendrimer with specific sites of the HSA protein. Curry *et al.*[27] have determined the crystal structure of complexes (5:1) of myristic acid with HSA. They confirmed that HSA has five different binding sites for carboxylic acids consisting of hydrophobic pockets capped by positively charged amino residues, for example, lysine (Lys) and arginine (Arg). As discussed by Diallo *et al.*,[28] the pK_a of the internal tertiary amine groups (p$K_a^{R_3N}$) and the pK_a of the pK_a^{RCOONa}) of the terminal carboxylic groups of the G3.5-COONa PAMAM are, respectively, equal to 6.30−6.85 and 4.5. Thus, the terminal carboxylic groups of the G3.5 PAMAM dendrimer are unprotonated and negatively charged (COO^-), whereas its internal tertiary amine groups are unprotonated and neutral in aqueous solutions at physiological pH (7.4). This suggests that the G3.5 PAMAM binds to HSA primarily through electrostatic interactions between its COO^- groups and the positively charged amino-acid residues of the carbolyxic acid binding sites of the protein.[27]

Finally, we would like to mention that the magnitude of the HSA binding constant (4.62 ± 1.21 × 10^6 M^{-1})

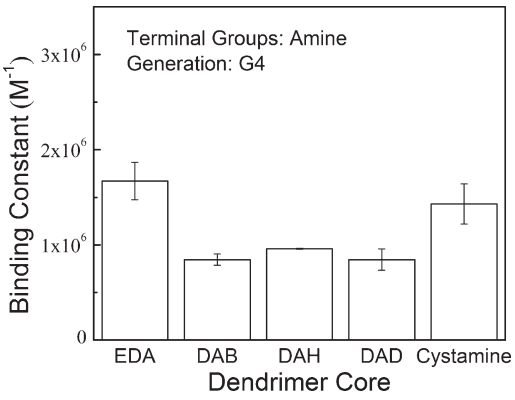

Figure 4. Effect of dendrimer core chemistry on the HSA binding (K_b) of G4 PAMAM dendrimers (G3.5 for Na−carboxylate) at room temperature and pH 7.4. In all cases, the concentration of dendrimer NH_2 groups was kept constant at 64 μM.

TABLE 3. Binding Constant K_b and Other Physical Parameters of G4 PAMAM Dendrimers with Different Cores

core[a]	terminal group	$N_{Terminal}$ [b]	M_{wth} (Da) [c]	K_b (M^{-1})
EDA	amine	64	14215	$1.67 \pm 0.19 \times 10^6$
DAB	amine	64	14277	$8.45 \pm 0.50 \times 10^5$
DAH	amine	64	20619	$9.59 \pm 0.05 \times 10^5$
DAD	amine	64	26252	$8.38 \pm 0.04 \times 10^5$
Cyst	amine	64	18121	$1.43 \pm 0.17 \times 10^6$

[a] EDA (ethylene diamine), DAB (diaminobutane), DAH (diaminohexane), DAD (diaminododecane), and Cyst (cystamine). [b] $N_{Terminal}$: number of terminal groups. [c] M_{wth}: theoretical molar mass.

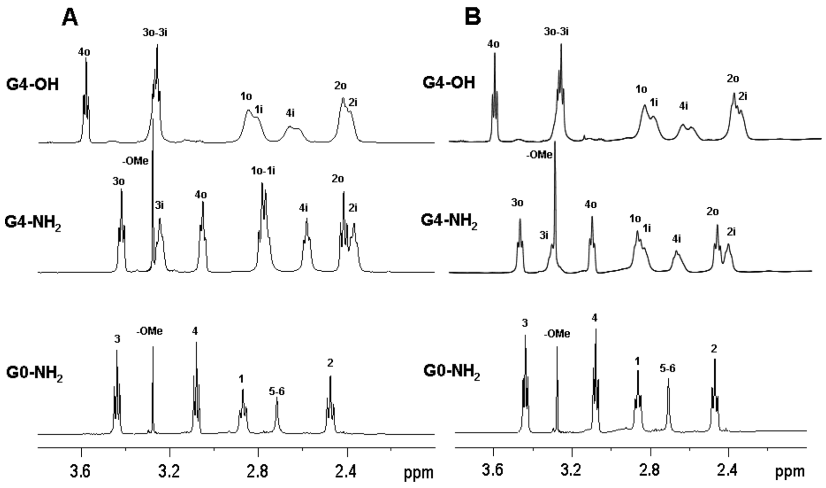

Figure 5. ^{1}H NMR of (A) PAMAM dendrimers, (B) PAMAM dendrimers + HSA complexes. Assignments were made from a series of 1D and 2D experiments (see the section Experimental and Computational Methods for more information). The proton labeling scheme is shown in Figure S6 of the SI. Note the dendrimers are highly symmetrical, thus proton 17 is also equivalent to 8, 13, and 21. The same applies to all other assignments. Where resolved, protons from the inner shells are labeled (i) and from the outer shell labeled (o). −OMe represents residual methanol solvent. Readers should note that signals from HSA are not clearly visible in the region shown as the heterogeneous and rigid structure of HSA results in high chemical shift dispersion (0−10 ppm) and relatively broad signals. In comparison the dendrimer have a more homogeneous repeating structure that gives rise to discrete NMR lines that swamp the more dispersed signals from the HSA even at a 1:1 molar ratio.

for the G3.5 PAMAM further supports the absence of specific interactions between dendrimers and the silica particles of the HSA-coated Transil beads.[22] At physiological pH (7.4), silica particles are negatively charged. If there were specific interactions between dendrimers and bare TRANSIL silica particles, one would expect the positively charged dendrimer (G4-NH_2 PAMAM) to exhibit a larger HSA binding constant than the negatively charged dendrimer (G3.5-COONa PAMAM) with comparable size and same number of terminal groups. However, we find that the K_b value of the G3.5 PAMAM ($4.62 \pm 1.21 \times 10^6\ M^{-1}$) is approximately 2 times larger than that of the G4-NH_2 dendrimer ($1.67 \pm 0.15 \times 10^6\ M^{-1}$). Figure 4 and Table 3 highlight the effects of core chemistry on the HSA binding constants of G4-NH_2 PAMAM dendrimers. Four different dendrimer cores were evaluated: ethylene diamine (EDA), diaminobutane (DAB), diaminohexane (DAH), diaminododecane (DA), and cystamine (Cys). The corresponding fractional binding curve is plotted in Figure S4 of the SI. We found no significant variation of dendrimer HSA binding constant with core chemistry.

NMR Investigations. Although binding constants can provide valuable information on the relative strengths of dendrimer−HSA complexes, no reliable information about molecular interactions can be derived from binding constant measurements alone. We used NMR spectroscopy to probe the interactions of PAMAM dendrimers with HSA in D_2O at physiological pD of 7.4.[29,30] Recall that albumin-coated TRANSIL beads contain polymer cushions that shield the immobilized HSA proteins from the silica particles while maintaining their conformational integrity.[22] Thus, we expect no significant difference between the interactions of PAMAM dendrimers with free and immobilized HSA proteins in aqueous solutions. Three model dendrimers were evaluated during the NMR experiments: G0-NH_2, G4-NH_2, and G4-OH (amidoethanol) PAMAM dendrimers with EDA core. For the G4 PAMAM dendrimers, 5 mg of dendrimer was mixed with 20 mg of protein to achieve an HSA−dendrimer molar ratio of 1.0. We initially tested an equimolar mixture of G0-NH_2 and HSA. However, the signals from the dendrimer could not be distinguished from the protein background signals due to the very low amount of G0-NH_2 PAMAM (0.16 mg) needed in this case to achieve a molar ratio of dendrimer−HSA of 1.0. We subsequently mixed 5 mg of G0-NH_2 PAMAM with 20 mg of HSA. In this case, the dendrimer−HSA molar ratio was equal to 32.0. Figure 5 compares the ^{1}H NMR spectra of the PAMAM dendrimers (A) and their mixtures with HSA (B). We observe little changes in the chemical shifts or line shapes of the ^{1}H NMR spectra of the G0-NH_2 dendrimer following the addition of HSA. This indicates that the local chemical environments of the dendrimer protons are relatively unaffected by the addition of HSA thereby suggesting that the interactions between HSA and the G0-NH_2 PAMAM are relatively weak and/or in fast exchange.[31] Owing to molar excess of the G0-NH_2 dendrimer, it is possible that the perturbations in chemical shifts induced by HSA−dendrimer interactions are masked by the free dendrimers. However, the DOSY experiments (Figure 6) clearly suggest that the interactions between HSA and the G0-NH_2 PAMAM are weak and/or highly dynamic in solution. Note also that the weak interactions between the G0-NH_2 PAMAM and HSA are consistent with the results of the EPR studies carried by Ottaviani *et al.*[26] They observed that the EPR spectra of

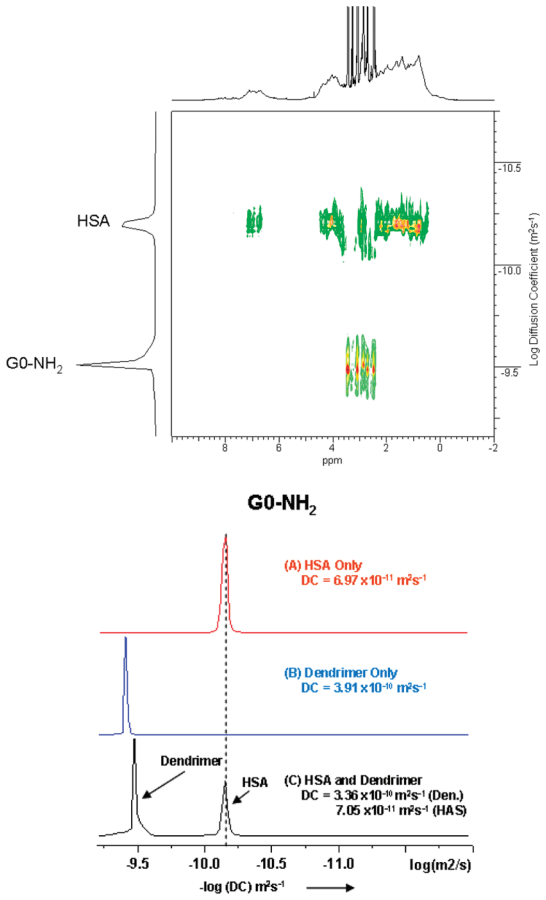

Figure 6. 2-D ^{1}H DOSY spectrum and projected diffusion profiles of G0-NH_2, HSA, and G0-NH2 + HSA complex in D_2O at pH 7.4.

HSA complexes with the G2-NH_2 PAMAM are "quite similar" to those of the dendrimer in D_2O. For the G4-NH_2 PAMAM dendrimer, we observed significant chemical shifts to lower fields for all resonances of the following addition of HSA (Figure 5). This suggests that all the dendrimer protons are exposed to different chemical environments, an indication of interactions between HSA and the G4-NH_2 PAMAM. These interactions are also consistent with the noticeable broadening[32] of the peaks of the dendrimer protons in the presence of HSA (Figure 5) as most clearly seen for protons 4i, 1o, and 1i (see Figure S6 of the SI for the labeling of the protons). We also observed small chemical shifts in all the resonances of the G4-OH dendrimer following addition of HSA (Figure 5). This suggests the interactions of HSA with the G4-OH dendrimer are weaker than those with the G4-NH_2 dendrimer. These results are consistent with the binding constant measurements, which show that the HSA binding constant of the G4-NH_2 dendrimer ($1.67 \pm 0.19 \times 10^6$ M^{-1}) is approximately 2 orders of magnitude larger than that of the G4-OH dendrimer ($1.29 \pm 0.93 \times 10^4$ M^{-1}).

We carried out diffusion ordered spectroscopy (DOSY) NMR experiments[31] to measure the diffusion constants of the PAMAM dendrimers, HSA, and their complexes. Figure 6 shows the 2-D ^{1}H spectra and projected diffusion profiles of the HSA (A), G0-NH_2 dendrimer (B), and HSA-dendrimer complex (C). The different regions of the NMR spectra of Figure 6 are well resolved and separated; thus highlighting a significant difference between the diffusion coefficients of the G0-NH_2 PAMAM and HSA. Note the small decrease in the diffusion coefficient of the G0-NH_2 dendrimer in the presence of HSA (Figure 6). The small decrease of the diffusion coefficient of the G0-NH_2 PAMAM also suggests that its interactions with HSA are weak, dynamic,[30] and fast during the time scale (~200 ms) of NMR DOSY experiments. We found that the DOSY diffusion profiles of the G4-NH_2 dendrimers are similar to that of HSA (data not shown). Because of this, we were unable to extract reliable diffusion coefficients for the dendrimer–HSA complexes due to the overlap between the diffusion peaks of the dendrimer and protein macromolecules.

We employed saturation transfer difference (STD) to probe the mechanisms and strengths of the interactions between PAMAM dendrimers and HSA. STD is commonly referred to as NMR epitope mapping.[32−35] A typical STD NMR experiment begins with the selective saturation of the host, HSA in this case. Saturation is then transferred to the guest molecules (*i.e.,* dendrimers in this case) that are interacting with the HSA macromolecules. During an STD experiment, the dendrimer protons closest to an HSA protein receive the greatest amount of saturation while those furthest from the protein receive the least. Note that only the interacting dendrimers are detected during an STD experiment while all other signals (*e.g.,* water or non-interacting dendrimers) cancel and are not observed (see the section Experimental and Computational Methods). Thus, the quantitative information about the strengths of the underlying molecular interactions between dendrimer and HSA macromolecules become encoded into the integrals of the dendrimer signals in a ^{1}H NMR STD spectrum. Figure 7 compares the epitope maps of the interactions of HSA with the G0-NH_2, G4-NH_2. and G4-OH PAMAM dendrimers. In an NMR epitope map, the percentage value for each type of proton represents an interaction strength that has been normalized by that of the strongest interacting proton, which is assigned a value of 100%. Note also that the % value for each proton is an "indirect" measure of the relative interaction strength of the functional groups in close proximity to the proton. In the case of the G0-NH_2 dendrimer (Figure 7A), we find that proton 2 adjacent to the CO of the amide group interacts more strongly with HSA. Surprisingly, the protons adjacent to the dendrimer NH_2 groups (*i.e.,* those protons attached to position 4) show the weakest interactions.

Figure 7B,C show the epitope maps of the interactions between HSA and the G4-NH_2 and G4-OH PAMAM

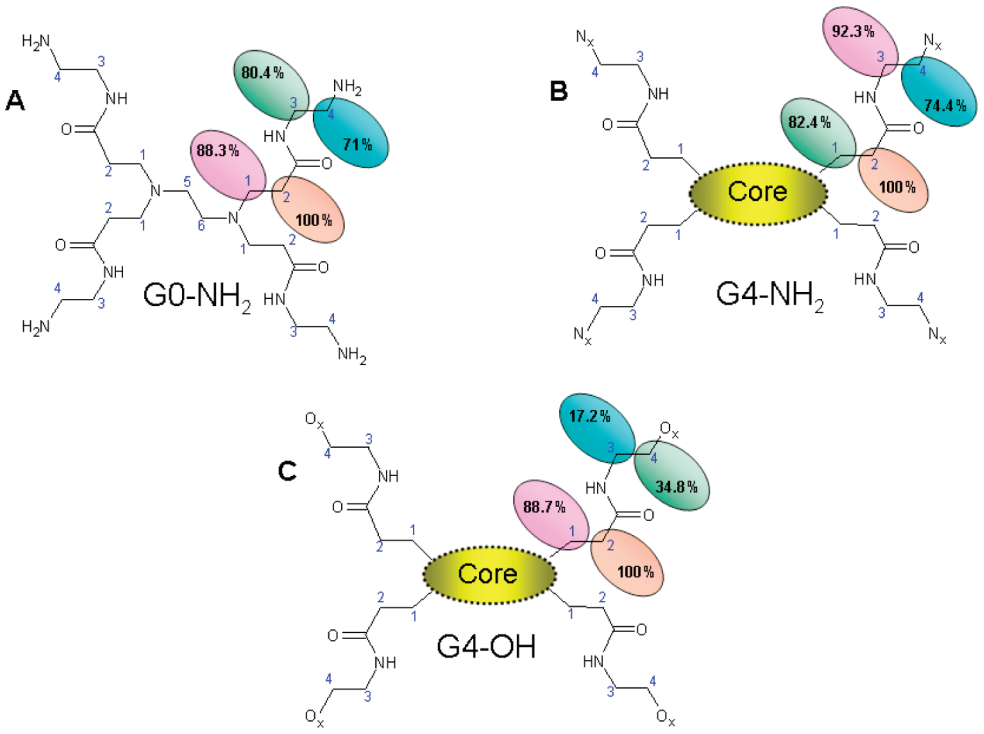

Figure 7. Epitope maps for the three dendrimers created from STD NMR (A–C). The percentage values for each epitope map are all relative to the strongest binding proton in each dendrimer, which is expressed as 100%. Red indicates the strongest interacting proton, pink the second, green the third, and blue the weakest. Only one branch of the dendrimers has been labeled for clarity but readers should understand that the interactions apply equally to all branches. Note only interactions from nonexchangeable protons can be measured in ^{1}H NMR STD experiments.

dendrimers. Figure S5 of the SI displays a 2-D structure of the G4-NH_2 PAMAM dendrimer with CH_2 groups labeled as 1, 2, 3, and 4. In Figure S5 of the SI, the terminal groups of the dendrimer outside the dashed circle are assigned to the outer shell, while the other groups within the dashed circle are assigned to the inner shells. Because of spectral overlaps, we could not generate the epitope maps of each specific dendrimer shell. Note that the protons at position 2 adjacent to the CO of the amide groups of the G4-NH_2 and G4-OH dendrimers also display the strongest interactions (Figures 7B and 7C). Figure 7C also shows the protons adjacent to the OH groups (protons 3 and 4) of the G4-OH PAMAM display weaker interactions. These weaker interactions are consistent with the lower HSA binding constant of this dendrimer and strongly suggest that the OH groups do not drive the interactions with the protein in the case of the G4-OH dendrimer. For all the G4-X dendrimers, we find a significant enhancement of signals of the protons from the dendrimer inner shells compared to those from the dendrimer outer shells. While these observations cannot be completely quantified to produce separate epitope maps for each specific dendrimer inner and outer shells, Figure S6 of the SI clearly shows that the inner protons receive more saturation from the protein (*i.e.*, stronger interactions) and thus are more enhanced in the difference spectrum than the corresponding outer shell protons.

Atomistic Molecular Dynamic Simulations. The overall results of the NMR epitope mapping experiments suggest that protons from the inner shells of the G0-NH_2, G4-NH_2, and G4-OH PAMAM dendrimers interact more strongly with HSA proteins. To get a molecular level insight into dendrimer–HSA interactions, we carried out atomistic molecular dynamics (MD) simulations to estimate the "contact" areas between the interacting protons of the dendrimer and HSA. We selected the G4-NH_2 PAMAM dendrimer as a model system and performed MD simulations to predict the structure and conformation of this dendrimer in water at physiological pH.[36] Figure 8 displays the equilibrated structure of the G4-NH_2 PAMAM dendrimer. The atom coloring schemes used in Figure 8 are the same as those in the epitope maps (Figure 7) obtained from the NMR experiments. We employed the solvent accessible surface areas (SASA)[37] of the equilibrated macromolecule (Figure 8) to estimate the relevant "contact" areas between the G4 PAMAM and HSA. The partial solvent accessible surface areas (PSASA) were calculated by decomposing the total SASA of the dendrimer into components for each relevant chemical group. Several probe radii (p = 1.4, 3, 6, 12, 24, and 48 Å) were employed in these calculations to mimic interacting molecules ranging from water to large protein macromolecules such as HSA. The van der Waals (vdW) radius of HSA (12 Å) was estimated using the radial

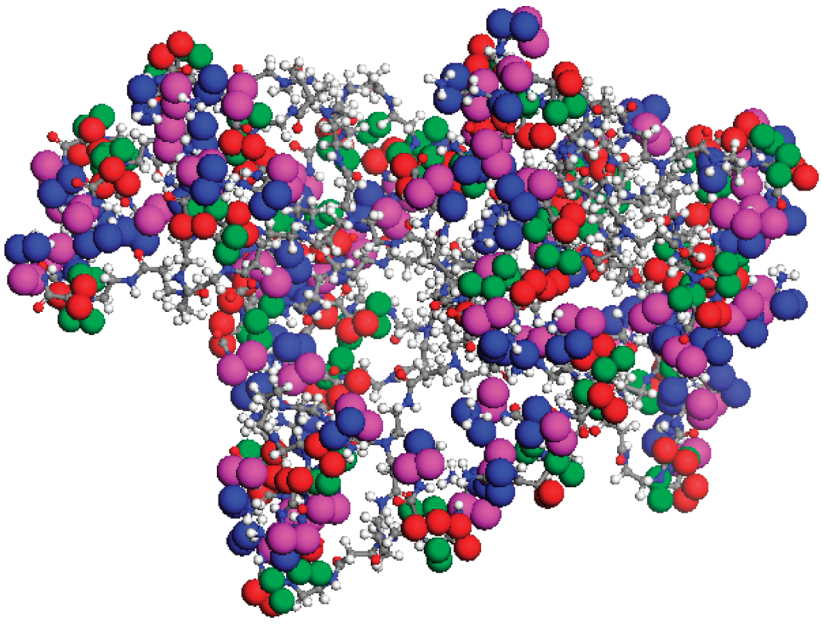

Figure 8. Atomic structure of a G4-NH_2 PAMAM dendrimer in aqueous solutions at neutral pH (snapshot taken from MD trajectory). The atom coloring schemes are the same as those in the epitope maps (Figure 7B) obtained from the NMR experiments: H1 (red balls) and H2 (green balls) represent the inner shell protons, whereas H3 (pink balls) and H4 (blue balls) represent the outer shell protons. The remainder of the dendrimer atoms are represented as ball-and-sticks.

distribution function of a HSA macrmolecule in the protein crystal structure (see Figure S7 of the SI).[38] Figure 9 shows the calculated PSASA values using p = 12 Å. Consistent with the proton labeling scheme used in Figure 7B, we denote the nonexchangeable protons of the G4-NH_2 PAMAM as H1, H2, H3, and H4, respectively, when they are connected to the CH_2 next to a primary amine, the CH_2 next to an amide CO, the CH_2 next to an amide NH, and the CH_2 next to a tertiary amine. Figure 9 shows the normalized PSASA of the protons of the CH_2 groups of the G4-NH_2 PAMAM relative to H2, which has been assigned a value of 100% as in the NMR STD spectrum (Figure 7B). The relative strength of interactions between the G4-NH_2 PAMAM and HSA estimated from the NMR epitope mapping experiments (Figure 7B) is shown for comparison. Table S1of the SI lists the calculated PSASA. When the probe radius is equal to the van der Waals (vdW) radius of HSA (12 Å), we find that the calculated PSASA for the G4-NH_2 PAMAM are equal to 58.4% for H1, 100.0% for H2 (reference), 94.3% for H3, and 77.3% for H4. These values correlate well with the estimated interaction strengths from the NMR epitope mapping experiments (Figure 4B): 82.4% for H1, 100.0% for H2 (reference), 92.3% for H3, and 74.4% for H4 (Figure 4B). Thus, the PSASA analysis predicts the correct trend of the interaction strengths found in the NMR experiments except for those of H1 and H4. We attribute this discrepancy mainly due to the spatial distribution of chemical groups of the dendrimer as discussed below.

Recall that NMR epitope mapping experiments can only "measure" interaction strengths averaged over all chemical groups of the entire guest. To obtain molecular

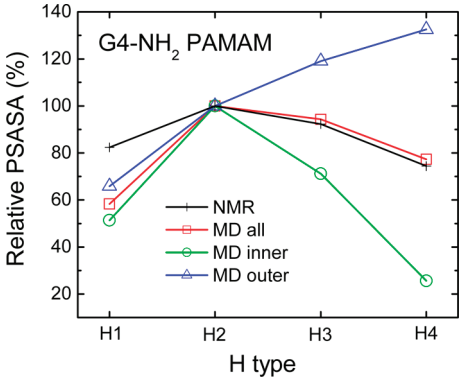

Figure 9. 3-D Partial solvent accessible surface area (PSASA) of the protons of CH_2 groups of G4-NH_2 PAMAM dendrimer relative to H2 (defined as 100) calculated in the MD simulations. The relative strength of interactions between G4-NH_2 PAMAM and HSA calculated from the NMR epitope mapping experiments is shown for comparison. A probe radius p = 12 Å, corresponding to the vdW radius of a HSA molecule, is used. H1−H4 represent the protons of the CH_2 groups defined in the same way as those in the epitope maps (Figure 7B) in the NMR experiments. The hydrogen atom type goes outward topologically in the order of H1, H2, H3, and H4.

level information about the groups of the G4-NH_2 PAMAM that interact with HSA, we computed the PSASA for the inner shell and outer shell protons of the dendrimer. In this case, the outer shell protons refer to protons that are connected to the dendrimer terminal NH_2 groups; whereas the inner shell protons refer to all protons from the remainder of the G4-NH_2 PAMAM excluding its EDA core (see Figure S5 of the SI). Figure 9 shows the calculated PSASA of the inner shell and outer shell protons (H1−H4) of the G4-NH_2 PAMAM. We find that the PSASA values of the outer shell

protons of the dendrimer increase as H1 < H2 < H3 < H4, which follows the trend expected from an ideal (topological) branched macromolecule. Note that the PSASA values of the inner shell protons of the G4-NH_2 PAMAM reach a maximum value for H2. Similarly, the sum of the PSASA values for all inner and outer shell protons of the G4-NH_2 PAMAM reaches a maximum value for H2. This suggests that the predicted PSASA trend from the MD simulations agree with the trend of the NMR interaction strengths only if the contributions of the inner shell protons are included, thus indicating the importance of HSA interactions with dendrimer inner shell protons. This result is consistent with the STD NMR spectra (Figure 8A), which show significant enhancement of the signals of the inner shell protons of the G4-NH_2 PAMAM following the addition of HSA.

Although the magnitudes of the contact areas can provide insightful information, we expect the spatial distributions of the groups of G4-NH_2 PAMAM to also affect their interactions with HSA. To test this hypothesis, we computed the partial radial mass density distributions of the protons of the CH_2 groups of G4-NH_2 PAMAM, using its center of mass as reference. Figure 10 shows the calculated partial radial density distributions averaged over 200 ps of the MD simulation trajectories. We found that H1 and H2 are distributed more outward than H3 and H4; whereas H3 exhibits a maximum density at a radial distance r = 16.5 Å, which is lower than those of H1, H2, and H4 at r = 19.5 Å. The maximum density for H4 (4.8 kg/m^3) is much smaller than that of H1 (6.0 kg/m^3) and H2 (6.1 kg/m^3). For an ideal (topological) G4-NH_2 PAMAM, we expect the protons to distribute more outwardly in the order H1 < H2 < H3 < H4. The abnormal proton distributions found from the MD simulations are consistent with the backfolding of the terminal amine groups of the G4-NH_2 PAMAM as discussed by Liu *et al.*[36] Our calculated radial distributions (Figure 10) indicate that the H1 and H2 protons and their neighboring amide CO groups are more exposed and/or closer to the solvent or protein molecules than the H3 and H4 protons and their neighboring amide NH or primary amine groups. This binding scenario is consistent with the trend found in the NMR epitope mapping experiments. The overall results of the binding measurements, NMR epitope mapping experiments and atomistic simulations suggest PAMAM dendrimers form weak complexes with HSA in aqueous solutions at physiological pH 7.4. These results are consistent with the EPR studies of the interactions of PAMAM dendrimers with amino acids and HSA in aqueous solutions published by Ottaviani *et al.*[26]

Biological Implications. As discussed in the introductory section, the binding of plasma proteins to nanoparticles (NPs) can significantly alter their *in vivo* transport in biological fluids. The formations of protein coatings on the surfaces of NPs have a significant impact on their fate in biological fluids as the proteins undergo conformational changes and/or dynamic exchanges with other proteins.[8,9] Because the magnitude of the hydrodynamic diameter of HSA (8 nm) at physiological pH (7.4) is comparable to those of G*x*-NH_2 PAMAM dendrimers (2–10 nm) [Table 1], there are significant differences between the structures and dynamics of dendrimer–HSA complexes and HSA-coated NPs. For example, Lindman *et al.*[39] found that HSA forms dense coronas consisting of 53 protein macromolecules on the surfaces of copolymeric (*N*-iso-propylacrylamide/*N*-*tert*-butylacrylamide) NPs (120 nm in diameter) in aqueous solutions at physiological pH (7.5). Conversely, Shcharbin *et al.*[19] have shown that HSA proteins form 1:5 complexes with G4-NH_2 PAMAM dendrimers. Several recent studies have established that dendrimer–protein complexes have a significant impact on a number of important biological processes.[24,40,41] For example, PAMAM dendrimers can serve as inhibitors to protein–protein binding and agggregation.[24,38] Protein aggregates such as amyloid fibril assemblies play a critical role in neurodegenerative diseases including Alzheimer's and prion (mad-cow) diseases.[40] Note that Klajnert *et al.*[41] have found that G5-NH_2 PAMAM dendrimers bound to HSA proteins are "significantly less harmful to red blood cells" than the bare G5 dendrimers. Conversely, Shcharbin *et al.*[42] have reported that PAMAM dendrimers can inhibit or enhance the activity of acetylcholinesterase (AChE) depending on their concentration and terminal group chemistry. AChE is a membrane bound enzyme that plays a key role in neurotransmission and signal transduction.[42] Collectively taken together, these data and the overall results of our investigations of dendrimer interactions with HSA suggest that the hypothesis Dawson and co-workers[12] might not be applicable to dendrimers with size comparable to those of plasma

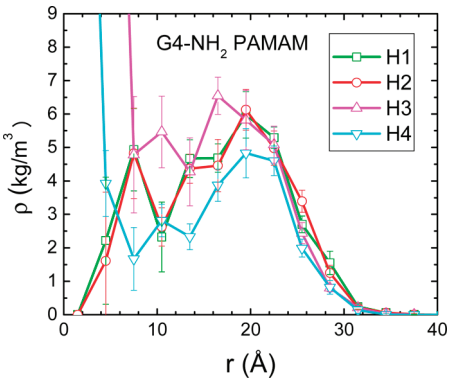

Figure 10. Partial radial density distributions of the protons of CH_2 groups of G4-NH_2 PAMAM dendrimer at neutral pH (averaged over 200 ps of MD trajectory). The atom labeling schemes H1–H4 are adopted as same as those in the epitope maps [Figure 7B] obtained from the NMR experiments. The hydrogen atom type goes outward topologically in the order of H1, H2, H3, and H4. The center of mass of the dendrimer is used as the reference.

proteins. In this case, "what the cell sees" might not be a NP core surrounded by a corona of long-lived plasma-proteins as suggested by Dawson and co-workers.[12] In the case of PAMAM dendrimers, we hypothesize that a cell will "*see*" and interact with weakly bound and dynamics protein-dendrimer complexes. We expect to learn more about the structures and functions of dendrimer-protein complexes as advances are made in the science and application of dendrimer nanotechnology to nanomedicine and nanobiotechnology.

CONCLUSIONS

This article describes an integrated experimental and computational modeling study of the interactions of poly(amidoamine) with human serum albumin (HSA) in aqueous solutions at physiological pH (7.4). We used protein-coated silica particles to measure the HSA binding constants (K_b) of a homologous series of 19 PAMAM dendrimers as a function of dendrimer generation, terminal group, and core chemistry. To gain insight into the mechanisms of HSA binding to PAMAM dendrimers, we combined ^{1}H NMR, saturation transfer difference (STD) NMR and NMR diffusion ordered spectroscopy (DOSY) of dendrimer-HSA complexes with atomistic molecular dynamics (MD) simulations of dendrimer conformation in aqueous solutions. We found that the HSA binding constants (K_b) of PAMAM dendrimers depend on size and terminal group chemistry. The K_b values suggest several mechanisms of interactions between PAMAM dendrimers and HSA proteins including (i) electrostatic interactions between charged dendrimer terminal groups and protein residues, (ii) hydrogen bonding between dendrimer internal groups (*e.g.*, amide moiety where the carbonyl O act as donor and the amide H as acceptor), and protein amino acid residues, (iii) hydrophobic interactions between the nonpolar dendrimer and HSA groups, and (iv) specific interactions between dendrimer carboxylic groups and protein aliphatic acid binding sites. The NMR ^{1}H and DOSY experiments showed that the interactions between HSA and PAMAM dendrimers are relatively weak. The NMR STD experiments and MD simulations indicate that the inner shell protons of the dendrimers and their neighboring amide groups interact more strongly with HSA proteins. These stronger interactions, which are consistently observed for different dendrimer generations (G0-NH_2 *vs* G4-NH_2) and terminal groups (G4-NH_2 *vs* G4-OH), suggest that PAMAM dendrimers adopt backfolded conformations as they form weak complexes with HSA proteins in aqueous solutions at physiological pH (7.4). Finally, we would like to point out that in the case of dendrimers, "what the cell sees" might not be a NP core surrounded by a corona of long-lived plasma-proteins as suggested by Dawson and co-workers.[12] For the PAMAM dendrimers evaluated in this study, we hypothesize that a cell will "see" and interact with weakly bound and dynamics protein-dendrimer complexes.

EXPERIMENTAL AND COMPUTATIONAL METHODS

Materials. PAMAM dendrimers of different generations, core and terminal groups (Figure 1) were purchased [as methanol solutions or solids] from Dendritech, Sigma-Aldrich, and Dendritic Nanotechnologies. Essentially fatty acid free human serum albumin (HSA) was purchased from Sigma-Aldrich (USA). TRANSIL beads coated with HSA were purchased as suspensions [201 mM in 0.15 M solution of phosphate buffered saline (PBS)] from Sovicell (Leipzig, Germany). All materials were used as received.

Binding Constant Measurement Methods. The binding constants (K_b) of PAMAM dendrimers were determined by mixing suspensions of HSA-coated TRANSIL beads with dendrimers in 1.5 mL Eppendorf vials at room temperature. All dendrimer solutions and Transil suspensions were prepared in 0.015 M PBS solution (13.7 mM NaCl, 0.27 mM KCl, 0.43 mM Na_2HPO_4, 0.147 mM KH_2PO_4). In a typical binding assay, aliquots of dendrimers (dry solid or methanol-free solution) were mixed with PBS, HCl, or NaOH to prepare stock solutions with pH 7.4. Then, 60 mL of dendrimer stock solutions and differing volumes of TRANSIL bead suspensions were added to each vial. This was followed by the addition of PBS (pH 7.4) to prepare 600 mL of dendrimer solution + TRANSIL bead suspensions. In all experiments, the total concentration of dendrimer in each vial ($[dent]_{total}$) was kept constant at 64 μM of equivalent terminal groups. For example, this corresponds to a concentration of 1.0 μM for all G4 PAMAM dendrimers with 64 terminal groups. For each dendrimer, we varied the protein concentration in each vial (from 0.5 to 7.5 μM) to prepare four suspensions with different molar ratios of HSA–dendrimer equivalent terminal groups. The vials containing the samples (dendrimer and HSA in PBS), reference solutions (dendrimer in PBS), controls (HSA in PBS), and buffer solutions were subsequently placed on a LabQuake shaker (Barnstead Thermolyne) and slowly rotated for 60 min. After equilibration, the vials [with TRANSIL bead suspensions] were centrifuged at 5000 G for 10 min followed by 10000 G for 15 min. Aliquots of sample (supernatant), reference, and buffer solutions were analyzed using a UV spectrometer (model T60 from PG Instruments). The measured absorbance (wavelength of 203 nm) of each sample supernatant was corrected (by subtracting the absorbance of the corresponding control) and used to determine the equilibrium concentration of dendrimer in the aqueous phase ($[dent]_{free}$). Similarly, the measured absorbance of each reference solution was corrected (by subtracting the absorbance of the buffer solutions) and used to determine $[dent]_{total}$. The concentration of dendrimer bound ($[dent]_{bound}$) to the HSA ($[dent]_{bound} = [dent]_{total} - [dent]_{free}$) was determined by mass balance. The HSA–dendrimer dissociation constant (K_d) was estimated using eq 1.[23]

$$K_d = [dent]_{free} \frac{1 - \dfrac{[dent]_{tot} - [dent]_{free} f_{corr}}{[protein]_{tot}}}{\dfrac{[dent]_{tot} - [dent]_{free} f_{corr}}{[protein]_{tot}}} \quad (1)$$

where the f_{corr} is a correction factor estimated using eq 2:[22]

$$f_{corr} = \frac{V_{H_2O}}{V_{total}} = \frac{V_{total} - V_{bead}}{V_{total}} \quad (2)$$

In eqs 1 and 2, V_{total} is the total volume of the suspension and V_{bead} is the volume of the Transil beads. Equation 1 is derived from the well-known Scatchard-equation for a system with one binding-site. A detailed description of this derivation is given elsewhere.[21,23,43] In all cases, each reported K_d value is the average of four measurements with different molar ratios of HSA to dendrimer NH_2 groups. The overall binding constant ($K_b = 1/K_d$) is taken as the inverse of the dissociation constant (K_d). Each reported error is the standard deviation of the average of four measured K_b values.

Scanning Electron Microscopy. Aliquots of TRANSIL HSA supensions were deposited on a coverslip glass (10 mm diameter) and dried under vacuum overnight. After sputter coating with gold for 90 s, the Transil beads were imaged by scanning electron microscopy (SEM) at 20 kV using a FEI SIRION-SEM instrument.

NMR Spectroscopy. Three PAMAM dendrimers were evaluated in the NMR studies: G0-NH_2, G4-NH_2, and G4-OH. Human Serum Albumin (20 mg) was mixed with 5 mg of dendrimer and dissolved in D_2O. For studies where HSA and the dendrimers were studied in isolation, identical concentrations were prepared. All samples were adjusted using minimal quantities of NaOD/DCl such that a meter reading of 7.0 was obtained on an Accumet Basic (Fisher Scientific) pH meter fitted with a glass NMR pH probe (Wilmad). Note that this corresponds to a pD of 7.4 after correction.[30] In the case of the G4 dendrimers, the molar ratio of dendrimer is ~1:1. An equimolar mixture of the G0:HAS was initially tested; but the signals from the dendrimer could not be distinguished from the protein background because of the very low quantities of G0-NH_2 dendrimer required. As such 5 mg of G0-NH_2 dendrimer were used in the experiments reported. Note that in this case the G0-NH_2 dendrimer is present in molar excess. All NMR spectra were acquired using a Bruker Avance 500 MHz spectrometer equipped with a ^{1}H-BB−^{13}C Triple Resonance Broadband Inverse (TBI) probe fitted with an actively shielded Z gradient. Unless stated otherwise water suppression was carried out using presaturation utilizing relaxation gradients and echos (PURGE).[44] All assignments were made using a combination of 2D heteronuclear single quantum coherence (HSQC), heteronuclear multiple bond correlation (HMBC), correlation spectroscopy (COSY), and phase-modulated CLEAN chemical exchange spectroscopy CLEANEX-PM (data note shown).[45]

Diffusion ordered spectroscopy (DOSY) experiments were performed with a bipolar pulse longitudinal encode−decode sequence.[46] Scans (256) were collected at a temperate of 298 K, using a diffusion time of 200 ms, and 16384 time domain points. A 2.5 ms sine-shaped encoding/decoding gradient pulse was ramped from 0.98 to 49 gauss/cm in 16 linear increments. Solvent suppression in DOSY was achieved with a presaturation of the water resonance using a 60 W amplifier attenuated at 60 db. Spectra were apodized through multiplication with an exponential decay corresponding to 1 Hz line broadening in F2 dimensions, and a zero filling factor of 2. All DOSY spectra were processed using Bruker's Topspin v.2.1 with up to 3 exponentials fitted to each data point, noise sensitivity factor of 1, and spike suppression factor of 4. The 16 slices were projected onto 128 points to create the diffusion dimension in F1.

Saturation transfer difference (STD) experiments were carried out using the approach described by Mayer *et al.*[32,33] incorporating a Carr−Purcell−Meiboom−Gill filter of 50 ms to attenuate the protein signals and presaturation for solvent suppression. Residual protein signals were subtracted using a double difference approach.[32,33] Selective saturation of the protein was achieved by a train of 50 ms Gauss shaped pulses, truncated at 1%, and separated by a 100 μs delay; 40 selective pulses were applied, leading to a total length of the saturation train of 2.004 s. The on-resonance irradiation of the HSA was performed at a chemical shift of 0.82 ppm and off-resonance irradiation at 114 ppm, where HSA signals were not present. Selective irradiation was carried out using a very carefully calibrated effective field of 81 Hz. The spectra were subtracted internally *via* phase cycling after every scan using different memory buffers for on- and off-resonance irradiation; 12 288 scans were accumulated for each STD experiment. Reference spectra were recorded using the identical sequence with the exception that no irradiation power was applied and that the phase cycle was changed such that each of the 256 scans were additive. All experiments were performed with 32 768 time domain points, 256 dummy scans, and additional recycle delay of 100 ms (in addition to the saturation time). Spectra were apodized through multiplication with an exponential decay corresponding to 1 Hz line broadening in the transformed spectrum, and a zero filling factor of 2. Spectral subtractions to produce the double difference spectra were performed in the interactive mode of Topspin 2.1 (Bruker BioSpin Ltd.).

Computational Methods. Acid−base titration experiments have shown that the terminal NH_2 groups of Gx-NH_2 PAMAM are fully protonated at physiological pH (7.4); whereas their tertiary amines remain neutral.[36] Therefore, we built a G4 PAMAM model with all primary amines protonated at neutral pH. The PAMAM dendrimer was solvated with explicit water molecules (~42000) and Cl^- counterions (64) in a cubic periodic box with ~11 nm side length. The system was minimized and then heated to 300 K over 10 ps. We ran MD simulations in NPT ensemble at 300 K and 1 atm for 2 ns, followed by NVT MD at 300 K for 1 ns. In all these simulations, we used Dreiding III force field that was developed recently for accurate description of hydrogen bonding interaction in dendrimers.[36] The further details of computational model and simulations are described in ref 36.

Acknowledgment. This work was carried out at the California Institute of Technology (Caltech) and the University of Toronto at Scarborough. Funding for the Caltech work was provided by the Environmental Protection Agency (EPA STAR Grant RD832525), the National Science Foundation (CBET NIRT Award 0506951), and the Oak Ridge National Laboratory (6400007192, LDRD 05125). Funding for the University of Toronto work (NMR experiments) was provided by Natural Sciences and Engineering Research Council of Canada (NSERC, Strategic and Discovery Programs) and the Government of Ontario in the form of an Early Researcher Award (A.J.S.). M.S. Diallo was also supported by the KAIST EEWS Initiative (NT080607C0209721). W. A. Goddard III was supported partially by the KAIST World Class University (WCU) program (NRF-31-2008-000-10055).

Supporting Information Available: Additional figures and data as described in the text. This material is available free of charge *via* the Internet at http://pubs.acs.org.

Note Added after ASAP Publication: After this paper was published online April 1, 2011, a correction was made to the bottom panel of Figure 2, and the *y*-axes of Figures 2−4 were amended. The revised version was published April 12, 2011.

REFERENCES AND NOTES

1. Colvin, V. L. The Potential Environmental Impact of Engineered Nanomaterials. *Nat. Biotechnol.* **2003,** *21*, 1166–1170.
2. Nel, A.; Xia, T.; Madler, L.; Li, N. Toxic Potential of Materials at the Nanolevel. *Science* **2006,** *311*, 622–627.
3. Faunce, T.; Watal, A. Nanosilver and Global Public Health: International Regulatory Issues. *Nanomedicine* **2010,** *5*, 617–632.
4. Anderson, J. M. Biological Responses to Materials. *Annu. Rev. Mater. Res.* **2001,** *31*, 81–110.
5. Engel, M. F. M.; Visser, A.; van Mierlo, C. P. M. Conformation and Orientation of a Protein Folding Intermediate Trapped by Adsorption. *Proc. Natl. Acad. Sci. U.S.A.* **2004,** *101*, 11316–11321.
6. Gray, J. J. The Interactions of Proteins with Solid Surfaces. *Curr. Opin. Struct. Biol.* **2004,** *14*, 110–115.
7. Shen, M. C.; Garcia, I.; Maier, R. V.; Horbett, T. A. Effects of Adsorbed Proteins and Surface Chemistry on Foreign

Body Giant Cell Formation, Tumor Necrosis Factor Alpha Release and Procoagulant Activity of Monocytes. *J. Biomed. Mater. Res. Part A.* **2004,** *70A*, 533–541.
8. Cedervall, T.; Lynch, I.; Lindman, S.; Berggard, T.; Thulin, E.; Nilsson, H.; Dawson, K. A.; Linse, S. Understanding the Nanoparticle−Protein Corona Using Methods to Quantify Exchange Rates and Affinities of Proteins for Nanoparticles. *Proc. Natl. Acad. Sci. U.S.A.* **2007,** *104*, 2050–2055.
9. Lynch, I.; Cedervall, T.; Lundqvist, M.; Cabaleiro-Lago, C.; Linse, S.; Dawson, K. A. The Nanoparticle−Protein Complex as a Biological Entity; A Complex Fluids and Surface Science Challenge for the 21st Century. *Adv. Colloid Interface Sci.* **2007,** *134*−*35*, 167–174.
10. Cedervall, T.; Lynch, I.; Foy, M.; Berggad, T.; Donnelly, S. C.; Cagney, G.; Linse, S.; Dawson, K. A. Detailed Identification of Plasma Proteins Adsorbed on Copolymer Nanoparticles. *Angew. Chem., Int. Ed.* **2007,** *46*, 5754–5756.
11. Lundqvist, M.; Stigler, J.; Elia, G.; Lynch, I.; Cedervall, T.; Dawson, K. A. Nanoparticle Size and Surface Properties Determine the Protein Corona with Possible Implications for Biological Impacts. *Proc. Natl. Acad. Sci. U.S.A.* **2008,** *105*, 14265–14270.
12. Walczyk, D.; Bombelli, F. B.; Monopoli, M. P.; Lynch, I.; Dawson, K. A. What the Cell "Sees" in Bionanoscience. *J. Am. Chem. Soc.* **2010,** *132*, 5761–5768.
13. Klein, J. Probing the Interactions of Proteins and Nanoparticles. *Proc. Natl. Acad. Sci. U.S.A.* **2007,** *104*, 2029–2030.
14. Frechet, M. J.; Tomalia, D. A. *Dendrimers and other Dendritic Polymers*; Wiley and Sons: New York, 2001.
15. He, X. M.; Carter, D. C. Atomic-Structure and Chemistry of Human Serum-Albumin. *Nature* **1992,** *358*, 209–215.
16. Peters, T. J. *All about Albumin; Biochemistry, Genetics and Medical Applications*; Academic Press: San Diego, London, 1996.
17. Kurz, H.; Trunk, H.; Weitz, B. Evaluation of Methods to Determine Protein-Binding of Drugs—Equilibrium Dialysis, Ultrafiltration, Ultracentrifugation, Gel-Filtration. *Arzneim.-Forsch. Beih.* **1977,** *27*, 1373–1380.
18. Purohit, G.; Sakthivel, T.; Florence, A. T. The Interaction of Cationic Dendrons with Albumin and Their Diffusion through Cellulose Membranes. *Int. J. Pharm.* **2003,** *254*, 37–41.
19. Shcharbin, D.; Janicka, M.; Wasiak, M.; Palecz, B.; Przybyszewska, M.; Zaborski, M.; Bryszewska, M. Serum Albumins Have Five Sites for Binding of Cationic Dendrimers. *Biochim. Biophys. Acta, Proteins Proteomics* **2007,** *1774*, 946–951.
20. Froehlich, E.; Mandeville, J. S.; Jennings, C. J.; Sedaghat-Herati, R.; Tajmir-Riahi, H. A. Dendrimers Bind Human Serum Albumin. *J. Phys. Chem. B.* **2009,** *113*, 6986–6993.
21. Sovicell. Transil Albumin Binding Kits (http://www.sovicell.com/products-protein-binding.asp, accessed August 19, 2010).
22. Loidl-Stahlhofen, A.; Schmitt, J.; Noller, J.; Hartmann, T.; Brodowsky, H.; Schmitt, W.; Keldenich, J. Solid-Supported Biomolecules on Modified Silica Surfaces—A Tool for Fast Physicochemical Characterization and High-Throughput Screening. *Adv. Mater.* **2001,** *13*, 1829–1834.
23. Schuhmacher, J.; Kohlsdorfer, C.; Buhner, K.; Brandenburger, T.; Kruk, R. High-Throughout Determination of the Free Fraction of Drugs Strongly Bound to Plasma Proteins. *J. Pharm. Sci.* **2004,** *93*, 816–830.
24. Chiba, F.; Hu, T. C.; Twyman, L. J.; Wagstaff, M. Dendrimers as Size Selective Inhibitors to Protein−Protein Binding. *Chem. Commun.* **2008,** *36*, 4351–4353.
25. Tomalia, D. A. In Quest of a Systematic Framework for Unifying and Defining Nanoscience. *J. Nanopart. Res.* **2009,** *11*, 1251–1310.
26. Ottaviani, F. M.; Jockush, S.; Tuuro, N. J.; Tomalia, D. A.; Barbon, A. Interactions of Dendrimers with Selected Amino Acids and Proteins Studied by Continuous Wave EPR and Fourier Transform EPR. *Langmuir* **2004,** *20*, 10238–10245.
27. Curry, S.; Mandelkow, H.; Brick, P.; Franks, N. Crystal Structure of Human Serum Albumin Complexed with Fatty Acid Reveals an Asymmetric Distribution of Binding Sites. *Nat. Struct. Biol.* **1998,** *5*, 827–835.
28. Diallo, M. S.; Arasho, W.; Johnson, J. H., Jr.; Goddard, W. A., III. Dendritic Chelating Agents. 2. U(VI) Binding to Poly(amidoamine) and Poly(propyleneimine) Dendrimers in Aqueous Solutions. *Environ. Sci. Technol.* **2008,** *42*, 1572–1579.
29. Boisselier, E.; Ornelas, C.; Pianet, I.; Aranzaes, J. R.; Astruc, D. Four Generations of Water-Soluble Dendrimers with 9 to 243 Benzoate Tethers: Synthesis and Dendritic Effects on their Ion Pairing with Acetylcholine, Benzyltriethylammonium, and Dopamine in Water. *Chem.—Eur. J.* **2008,** *14*, 5577–5587.
30. Krezel, A.; Bal, W. A Formula for Correlating pK_a Values Determined in D_2O and H_2O. *J. Inorg. Biochem.* **2004,** *98*, 161–166.
31. Simpson, A. J. Determining the Molecular Weight, Aggregation, Structures and Interactions of Natural Organic Matter Using Diffusion Ordered Spectroscopy. *Magn. Reson. Chem.* **2002,** *40*, S72–S82.
32. Hu, J. J.; Cheng, Y. Y.; Ma, Y. R.; Wu, Q. L.; Xu, T. W. Host−Guest Chemistry and Physicochemical Properties of the Dendrimer−Mycophenolic Acid Complex. *J. Phys. Chem. B.* **2009,** *113*, 64–74.
33. Mayer, M.; Meyer, B. Characterization of Ligand Binding by Saturation Transfer Difference NMR spectroscopy. *Angew. Chem., Int. Ed. Engl.* **1999,** *38*, 1784–1788.
34. Mayer, M.; Meyer, B. Group Epitope Mapping by Saturation Transfer Difference NMR to Identify Segments of a Ligand in Direct Contact with a Protein Receptor. *J. Am. Chem. Soc.* **2001,** *123*, 6108–6117.
35. Shirzadi, A.; Simpson, M. J.; Xu, Y.; Simpson, A. J. Application of Saturation Transfer Double Difference NMR to Elucidate the Mechanistic Interactions of Pesticides with Humic Acid. *Environ. Sci. Technol.* **2008,** *42*, 1084–1090.
36. Liu, Y.; Bryantsev, V. S.; Diallo, M. S.; Goddard, W. A. PAMAM Dendrimers Undergo pH Responsive Conformational Changes without Swelling. *J. Am. Chem. Soc.* **2009,** *131*, 2798–2799.
37. Connolly, M. L. Solvent-Accessible Surfaces of Proteins and Nucleic-Acids. *Science* **1983,** *221*, 709–713.
38. Sugio, S.; Kashima, A.; Mochizuki, S.; Noda, M.; Kobayashi, K. Crystal Structure of Human Serum Albumin at 2.5 Angstrom Resolution. *Protein Eng.* **1999,** *12*, 439–446.
39. Lindman, S.; Lynch, I.; Thulin, E.; Nilsson, H.; Dawson, K. A.; Linse, S. Systematic Investigation of the Thermodynamics of HSA Adsorption to *N*-iso-propylacrylamide/*N*-*tert*-butylacrylamide Copolymer Nanoparticles. Effects of Particle size and Hydrophobicity. *Nano Lett.* **2007,** *7*, 914–920.
40. Klajnert, B.; Cortijo-Arellano, M.; Cladera, J.; Bryszewska, M. Influence of Dendrimer's Structure on Its Activity Against Amyloid Fibril Formation. *Biochem. Biophys. Res. Commun.* **2006,** *345*, 21–28.
41. Klajnert, B.; Pikala, S.; Bryszewska, M. Haemolytic Activity of Polyamidoamine Dendrimers and the Protective Role of Human Serum Albumin. *Proc. R. Soc. A.* **2010,** *466*, 1527–1534.
42. Shcharbin, D.; Jokiel, M.; Klajnert, B.; Bryszewska, M. Effect of Dendrimers on Pure Acetylcholinesterase Activity and Structure. *Bioelectrochemistry* **2006,** *68*, 56–59.
43. Scatchard, G. The Attractions of Proteins for Small Molecules and Ions. *Ann. N.Y. Acad. Sci.* **1949,** *51*, 660–672.
44. Simpson, A. J.; Brown, S. A. Purge NMR: Effective and Easy Solvent Suppression. *J. Magn. Reson.* **2005,** *175*, 340–346.
45. Hwang, T. L.; Mori, S.; Shaka, A. J.; van Zijl, P. C. M. Application of Phase-Modulated CLEAN Chemical EXchange Spectroscopy (CLEANEX-PM) to Detect Water-Protein Proton Exchange and Intermolecular NOEs. *J. Am. Chem. Soc.* **1997,** *119*, 6203–6204.
46. Wu, D. H.; Chen, A. D.; Johnson, C. S. An Improved Diffusion-Ordered Spectroscopy Experiment Incorporating Bipolar-Gradient Pulses. *J. Mag. Reson., Ser. A* **1995,** *115*, 260–264.